

## Step ordering induced by nonplanar patterning of GaAs surfaces

A. Dalla Volta and D. D. Vvedensky<sup>a)</sup>

*The Blackett Laboratory, Imperial College, London SW7 2BW, United Kingdom*

N. Gogneau, E. Pelucchi, A. Rudra, B. Dwir, and E. Kapon

*Laboratory of Physics of Nanostructures, Ecole Polytechnique Fédérale de Lausanne (EPFL), CH-1015 Lausanne, Switzerland*

C. Ratsch

*Department of Mathematics, University of California, Los Angeles, California 90095-1555*

(Received 28 November 2005; accepted 30 March 2006; published online 15 May 2006)

We report the observation and theory of the morphological evolution of vicinal (001) ridges on V-grooved GaAs surfaces during metal organic vapor-phase epitaxy. The pattern of the nonplanar substrate induces unusual ordering of monatomic steps, different from the free flow observed on a nonpatterned vicinal surface. The step edges develop profiles that kinetic Monte Carlo simulations reveal are determined by the width of the ridges between neighboring V grooves and the kinetics of interfacet mass migration between the ridge and the bounding sidewalls of the V groove. © 2006 American Institute of Physics. [DOI: 10.1063/1.2204441]

The lithographic patterning of surfaces exposes crystal-line facets with different chemical, transport, and structural properties. Accompanying such variations of *individual* facet properties is an interaction mediated by interfacet mass transfer. These factors conspire to produce a nonuniform growth rate across a patterned substrate that can be exploited to influence the positioning, size, and composition of heterostructures. This strategy has already produced uniform arrays of quantum wires and dots with metal organic vapor-phase epitaxy (MOVPE) and molecular-beam epitaxy (MBE) on substrates patterned with V grooves<sup>1,2</sup> and pyramidal recesses.<sup>3-5</sup>

In this letter, we report the observation and theory of an especially striking example of epitaxial growth on a patterned surface: the evolution of step trains with unusual morphologies on (001) ridges during MOVPE on V-grooved GaAs. Monatomic step ordering (with different profiles) during MOVPE on nonpatterned substrates has been reported previously,<sup>6</sup> but the underlying mechanisms have yet to be identified. By using atomic force microscopy (AFM) and kinetic Monte Carlo (KMC) simulations, we show that the observed step profiles provide direct evidence of diffusional mass flow from the facets bounding the ridge and of the presence of reflecting boundaries at the side facets. Our results establish a means of measuring the spatially resolved diffusional flow of mass across a patterned substrate and suggest the possibility of designing patterns that channel mass into predetermined regions of the substrate. This would improve the self-organization process and bring the notion of true selective area growth closer to fruition.

Planar GaAs(001) substrates were patterned by electron-beam lithography and selective wet chemical etching. The patterning consists of 600-nm-wide  $[01\bar{1}]$ -oriented V grooves separated by ridges whose widths vary from 0.1 to 10  $\mu\text{m}$  on a surface misoriented by  $\sim 0.05^\circ$  along the groove direction in the center of the substrate. Growth was carried out with low-pressure MOVPE at  $\sim 680^\circ\text{C}$  and a

growth rate of 0.20 nm/s in a horizontal reactor using trimethylgallium (TMGa) and  $\text{AsH}_3$  as source materials with  $\text{N}_2$  as the carrier gas. The morphology of the (001) ridges was characterized with AFM, scanned in air, which leads to the formation of a thin native oxide film. However, the step widths and heights are similar to those measured on nonoxidized surfaces.<sup>7</sup>

Figure 1 shows  $5 \times 5 \mu\text{m}^2$  flattened AFM images of steps on the upper GaAs(001) ridge as a function of its width  $W$ . For narrower ridges [Figs. 1(a)–1(c)] the steps are essentially straight and perpendicular to the bounding V grooves, but with substantial terrace length fluctuations, ranging from a few tenths of a micron to several microns. There is a tendency toward more regular spacings with increasing ridge width. For  $W=0.5 \mu\text{m}$  [Fig. 1(d)] the steps deviate from the straight profiles seen for narrower ridges. Increasing the ridge width further causes the terrace lengths to become more regular and the step profile to develop a pronounced concave undulation [Figs. 1(e) and 1(f)]. Step profile fluctuations are a strong function of  $W$ , showing a regular shape and terrace width for  $W=0.8 \mu\text{m}$ , but variations in both quantities are evident for the widest ridge ( $W=2.0 \mu\text{m}$ ).

Our simulations of the morphologies in Fig. 1 are based on the following schematic MOVPE sequence. TMGa and  $\text{AsH}_3$  arrive at the substrate by diffusion through a boundary layer, after which these species and any of their fragments migrate with minimal lateral interactions to step edges, where they release Ga and As through decomposition reactions.<sup>8</sup> The highly mobile surface species lead to step flow growth with terrace lengths of up to several microns, which preempts the direct simulation of growth in this system. However, in the absence of lateral interactions, adatom motion on the terraces and along the step edges can be expressed in terms of a dimensionless linear theory. Comparison to experimental length and time scales thereby provides estimates of diffusion and flux parameters. KMC simulations have been carried out on small systems in the knowledge that the parameters can be scaled to the experimental system.

KMC simulations<sup>10</sup> were carried out on simple cubic vicinal surfaces with the two main modifications caused by

<sup>a)</sup>Electronic mail: d.vvedensky@imperial.ac.uk

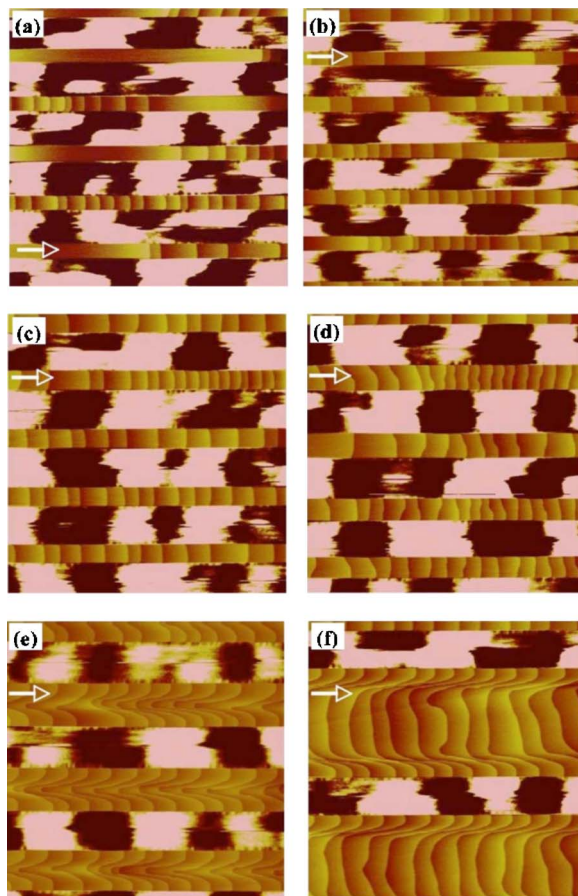


FIG. 1. (Color online)  $5 \times 5 \mu\text{m}^2$  flattened AFM images of step trains on a V-grooved vicinal GaAs(001) substrate. The ridge widths  $W$  are (a)  $0.1 \mu\text{m}$ , (b)  $0.2 \mu\text{m}$ , (c)  $0.4 \mu\text{m}$ , (d)  $0.5 \mu\text{m}$ , (e)  $0.8 \mu\text{m}$ , and (f)  $2.0 \mu\text{m}$ . The arrows indicate the step flow direction.

the patterning. (i) The steps approach the edges of the ridge at right angles. This suggests that an adatom or admolecule migrating along the step is reflected at the V-groove boundary back toward the interior of the ridge. According to Fick's first law, this translates into a vanishing derivative of the step-edge profile at the V groove. (ii) The higher dissociation rate of TMGa on the sidewalls of the  $\{111\}$  V groove than on the (001) ridge<sup>9</sup> produces a higher growth rate within the V groove, which leads to the planarization of the substrate. The concomitant lateral growth of the ridge is accompanied by the transfer of material from the sidewalls, which we include as an additional lateral flux to the ridge.

Periodic boundary conditions are imposed along the step train with reflecting boundary conditions in the lateral direction. Atoms are deposited randomly on the surface and at lateral edge sites at average fluxes  $J_0$  and  $J_e$ , respectively. Surface diffusion is modeled by nearest-neighbor hopping with rate  $\nu_0 \exp(-E_D/k_B T)$ , where  $\nu_0 \sim 10^{13} \text{ s}^{-1}$ ,  $k_B$  is Boltzmann's constant,  $T$  is the absolute temperature, and  $E_D = E_S + nE_N$  is the hopping barrier, given by a substrate term  $E_S$  and a contribution  $E_N$  from each of the  $n$  lateral nearest neighbors of the initial state. Atoms attached to a step can hop to a first- or second-neighbor site to maximize their coordination. This allows for step-edge diffusion. For  $E_S = 1.55 \text{ eV}$ ,  $E_N = 0.3 \text{ eV}$ ,  $T = 680 \text{ }^\circ\text{C}$ ,  $J_0 = 1 \text{ monolayer (ML)/s}$ , and  $J_e = 0.1 \text{ ML/s}$ , nucleation on the terraces is virtually absent on terraces of length  $10a$ .

Downloaded 05 Sep 2006 to 169.232.46.14. Redistribution subject to AIP license or copyright, see <http://apl.aip.org/apl/copyright.jsp>

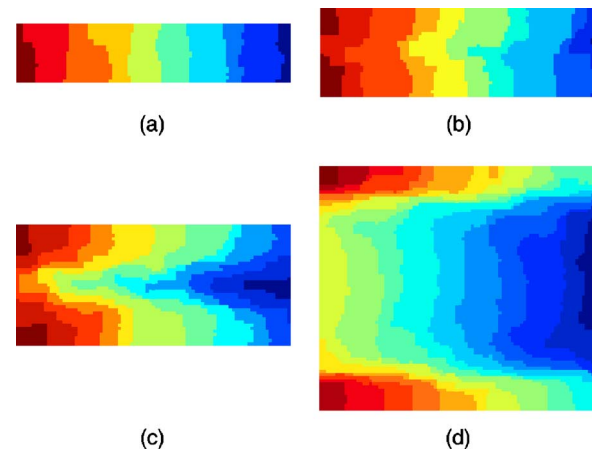


FIG. 2. (Color online) Morphologies produced by KMC simulations after the deposition of 8 ML (measured in units of  $J_0 t$ ) on a lattice with nine steps with an average terrace length of  $10a$  and widths of (a)  $20a$ , (b)  $30a$ , (c)  $40a$ , and (d)  $80a$ . The step flow direction is from left to right.

Figure 2 shows the simulated step morphologies for systems of length  $90a$  and ridge widths of  $20a$ ,  $30a$ ,  $40a$ , and  $80a$ , where  $a$  is the lattice constant. The trends in the step profiles closely follow those in Fig. 1: moderately straight steps with weak terrace length fluctuations for narrow ridges [Fig. 2(a)], developing large fluctuations in both profile and terrace length [Fig. 2(b)], and pronounced concave profiles with increasing depth for wider ridges [Figs. 2(c) and 2(d)]. In common with the measured morphologies, the direct influence of the V groove diminishes toward the center of the ridge over a characteristic distance that is independent of the ridge width, leading to a recessed profile in the center of the ridge.

If the V grooves are etched at an angle  $\beta$  with respect to the misorientation direction of the substrate, growth produces a realignment of the steps normal to the V grooves. A series of simulated morphologies is shown in Fig. 3 for  $W = 40a$ . The initial orientation of the steps is shown in Fig. 3(a). Even after a deposition time  $J_0 t = 1 \text{ ML}$ , the memory of the initial orientation has been largely lost. After the deposition of 8 ML [Fig. 3(d)], the morphology is indistinguishable from that in Fig. 2(c). The mechanism of this behavior can be understood by referring to Fig. 3(a). Each step is initially composed of a finite train of one-dimensional steps. Deposition causes these steps to advance by lateral "step flow" until the most distant step [at the lower boundary in Fig. 3(a)] has reached the far ridge boundary [the upper boundary in Fig.

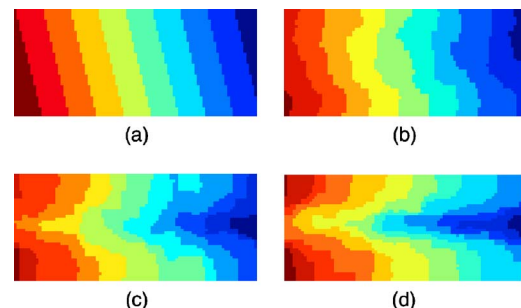


FIG. 3. (Color online) Evolution of morphologies produced by KMC simulations for V grooves etched at an angle with respect to the misorientation direction of the substrate, as shown in (a) on a lattice with nine steps with an average terrace length of  $10a$  and a width of  $40a$ . The steps are shown after the deposition times  $J_0 t$  of (b) 1 ML, (c) 4 ML, and (d) 8 ML.

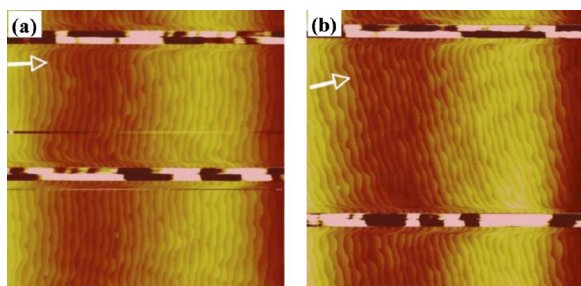


FIG. 4. (Color online)  $15 \times 15 \mu\text{m}^2$  flattened AFM images of step trains on a V-grooved vicinal GaAs(001) substrate. The ridge widths  $W$  are (a)  $5 \mu\text{m}$  and (b)  $10 \mu\text{m}$ . The arrows indicate the step flow direction in the center of the ridge.

3(a)]. Thereafter, the evolution of the steps is largely independent of the initial condition, as a comparison between Figs. 3(d) and 2(c) shows.

Based on this scenario, we estimate the time  $\tau$  for the steps to reorient along the V grooves as  $\tau \sim W \sin \beta / 2J_0 \ell$ ;  $\ell$  is the average distance between steps. For the parameters of the simulation in Fig. 3, we obtain  $\tau \sim 1 \text{ ML}$ , which is consistent with the morphology in Fig. 3(b). The reorientation time  $\tau$  increases with ridge width  $W$  and in Fig. 4 we show the manifestation of this on the step morphologies. For  $W = 5 \mu\text{m}$  [Fig. 4(a)], the steps have been completely reoriented by the V grooves. But, for  $W = 10 \mu\text{m}$  [Fig. 4(b)], the same deposition time does not produce the same degree of orientation.

In summary, we have reported AFM observations of unusual step ordering on ridges of GaAs(001) V-grooved vicinal substrates during MOVPE. KMC simulations with a lateral mass flux from the V grooves and reflecting boundaries

at the V grooves account for all of the observed morphological features. Understanding the underlying mechanisms of monolayer step morphologies during epitaxial growth on patterned substrates may pave the way for the preparation of quantum well and quantum wire heterostructures with improved interface morphology, which is important for the realization of low-dimensional electronic systems with near-ideal behavior.

This research was supported by funds from the Swiss National Science Foundation, the U.K. Engineering and Physical Sciences Research Council, and the European Commission Sixth Framework Programme as part of the European Science Foundation EUROCORES Programme on Self-Organized Nanostructures (SONS).

<sup>1</sup>S. Koshiba, H. Noge, H. Akiyama, T. Inoshita, Y. Nakamura, A. Shimizu, Y. Nagamune, M. Tsuchiya, H. Kano, H. Sakaki, and K. Wada, *Appl. Phys. Lett.* **64**, 363 (1994).

<sup>2</sup>A. Gustaffson, F. Reinhardt, G. Biasiol, and E. Kapon, *Appl. Phys. Lett.* **67**, 3673 (1995).

<sup>3</sup>A. Hartmann, L. Loubies, F. Reinhardt, and E. Kapon, *Appl. Phys. Lett.* **71**, 1314 (1997).

<sup>4</sup>S. Ishida, Y. Arakawa, and K. Wada, *Appl. Phys. Lett.* **72**, 800 (1998).

<sup>5</sup>S. Watanabe, E. Pelucchi, K. Leifer, A. Malko, B. Dwir, and E. Kapon, *Appl. Phys. Lett.* **86**, 243105 (2005).

<sup>6</sup>F. Reinhardt, B. Dwir, G. Biasiol, and E. Kapon, *J. Cryst. Growth* **170**, 689 (1997).

<sup>7</sup>C. C. Hsu, J. B. Xu, I. H. Wilson, T. G. Andersson, and J. V. Thordson, *Appl. Phys. Lett.* **65**, 1552 (1994).

<sup>8</sup>F. Lelarge, G. Biasiol, A. Rudra, A. Condo, and E. Kapon, *Microelectron. J.* **30**, 461 (1999).

<sup>9</sup>S. H. Jones and L. S. Salinas, *J. Cryst. Growth* **154**, 163 (1995).

<sup>10</sup>T. Shitara, D. D. Vvedensky, M. R. Wilby, J. Zhang, J. H. Neave, and B. A. Joyce, *Phys. Rev. B* **46**, 6815 (1992).